iScience

CellPress
OPEN ACCESS

Article

Pim-1 kinase protects the liver from ischemia reperfusion injury by regulating dynamics-related protein 1

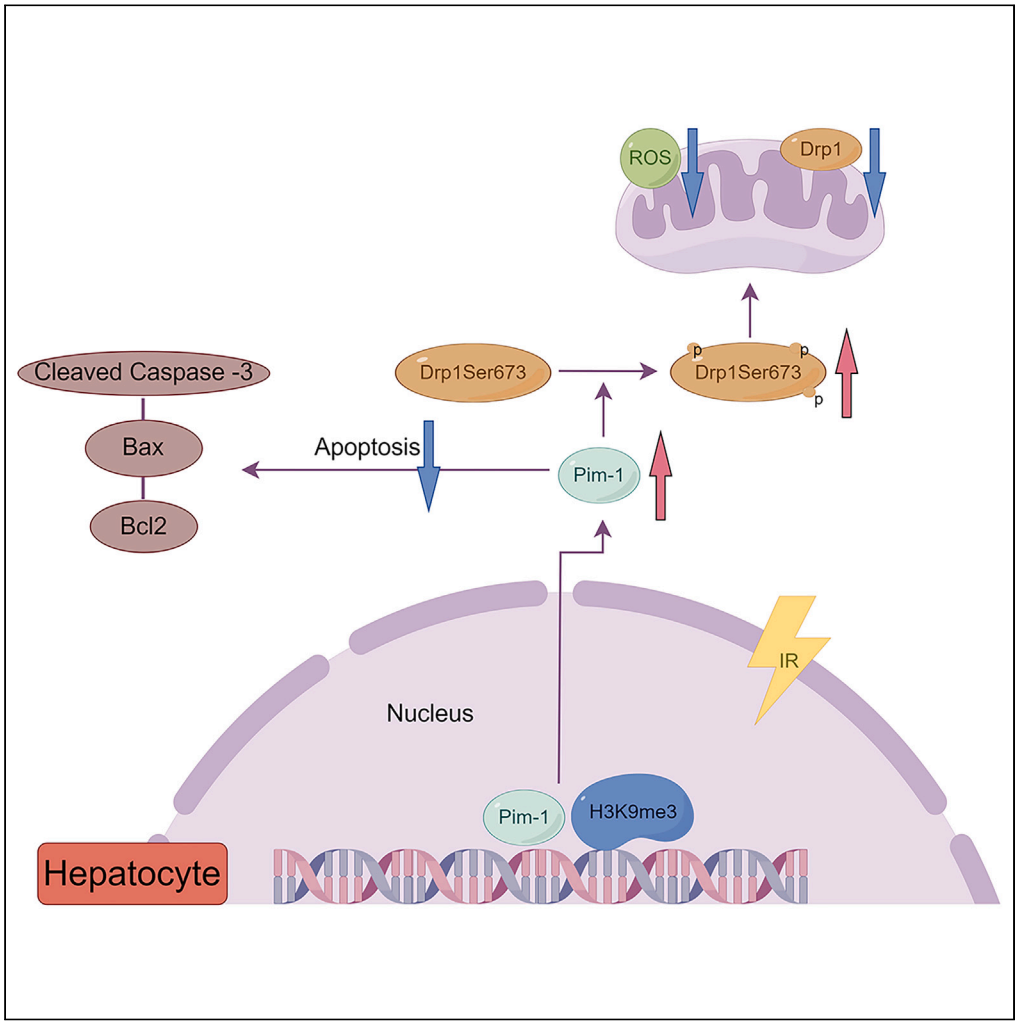

Yan-dong Sun, Qing-guo Xu, De-shu Dai, ..., Chuan-shen Xu, Bin Wu, Jin-zhen Cai

caijinzhen@qdu.edu.cn

Highlights

Pim-1 levels increase post-reoxygenation in MIHA cells

High Pim-1 correlates with better liver transplant recovery

Pim-1 inhibition raises necrosis in liver IR models

Pim-1 regulates Drp1, protecting mitochondrial integrity

Sun et al., iScience *27*, 110280
July 19, 2024
https://doi.org/10.1016/j.isci.2024.110280

iScience

CellPress
OPEN ACCESS

Article

Pim-1 kinase protects the liver from ischemia reperfusion injury by regulating dynamics-related protein 1

Yan-dong Sun,[1] Qing-guo Xu,[1] De-shu Dai,[1] Shu-xian Wang,[1] Xin-qiang Li,[1] Shang-heng Shi,[1] Peng Jiang,[1] Yan Jin,[1] Xin Wang,[1] Yong Zhang,[1] Feng Wang,[1] Peng Liu,[1] Bing-liang Zhang,[1] Tian-xiang Li,[1] Chuan-shen Xu,[1] Bin Wu,[1] and Jin-zhen Cai[1,2,*]

SUMMARY

Hepatic ischemia-reperfusion (IR) injury significantly impacts liver transplantation success, yet current treatments remain inadequate. This study explores the role of Proto-oncogene serine/threonine-protein kinase (Pim-1) in liver IR, an area previously unexplored. Utilizing a mouse liver IR *in vivo* model and a MIHA cell hypoxia–reoxygenation *in vitro* model, we observed that Pim-1 expression increases following IR, inversely correlating with serum alanine aminotransferase (ALT) and aspartate aminotransferase (AST) levels. Increased Pim-1 expression stabilizes mitochondrial membranes by modifying Drp1 phosphorylation, reducing mitochondrial fission and apoptosis, thereby mitigating liver damage. Additionally, we discovered that elevated Pim-1 expression is dependent on the trimethylation of histone H3 lysine 9 during liver IR. These findings underscore the importance and potential clinical application of targeting Pim-1 in treating hepatic IR, presenting a novel therapeutic avenue.

INTRODUCTION

Hepatic ischemia–reperfusion (IR) injury is a serious complication of various liver operations, such as liver transplantation and partial hepatectomy, and hemorrhagic shock.[1] Despite significant progress in recent years, hepatic IR remains one of the important causes of postoperative liver dysfunction and early liver failure following liver transplantation and leads to a poor prognosis for patients,[2] for which there is still no effective interventional treatment method.[3] Therefore, it is important to thoroughly investigate the underlying mechanisms of hepatic IR occurrence.

Mitochondria are dynamic organelles that provide cells with the energy necessary for survival. Under normal conditions, they are in a balance of fusion and fission. When ischemia–reperfusion damage occurs, mitochondrial homeostasis is disrupted, and fission tends to result.[4,5] Studies have shown that fissioned mitochondria cannot produce enough mitochondrial respiratory complexes, which leads to reduced oxidative phosphorylation and increased reactive oxygen species (ROS) production. In addition, damaged mitochondria can release proapoptotic factors and initiate mitochondria-dependent apoptosis pathways to further aggravate the damage.[6–8] Dynamics-related protein 1 (Drp1) is a key protein that regulates mitochondrial division. Ischemia and reperfusion can cause dephosphorylation of the Drp1 Ser637 site, promote the transfer of Drp1 to the outer mitochondrial membrane, and further lead to mitochondrial fragmentation and excessive release of cytochrome *c* to induce apoptosis.[9,10] Therefore, inhibiting mitochondrial fission or promoting mitochondrial fusion may represent a measure to reduce ischemia–reperfusion-related damage.

Proto-oncogene serine/threonine-protein kinase (Pim-1) belongs to the kinase family of Moloney murine leukemia virus proteins. Its function is to phosphorylate the serine and threonine sites of some proteins, and it plays vital roles in cell proliferation, differentiation, and survival.[11] Pim-1 is involved in the progression of liver cancer cells through the tri-methylation of histone H3 on the ninth lysine (H3K9me3).[12] Meanwhile, the accumulation of trimethylated histone H3K9 occurs during ischemia–reperfusion.[13] This indicates that the expression of Pim-1 may change during the process. Previous studies have shown that the cardioprotective effect of Pim-1 kinase is related to the stabilization of mitochondrial structure, upregulation of the antiapoptotic protein Bcl-2, promotion of cell survival, inhibition of myocardial hypertrophy, and fibrosis.[14,15] Recent studies have shown that Pim-1 attenuates ischemia–reperfusion injury by maintaining the stability of cardiomyocyte mitochondria during cardiomyocyte ischemia–reperfusion,[16,17] but its role in liver IR has not been reported. Therefore, in this study, we explored the role of Pim-1 in the process of liver IR to clarify its mechanism and to provide a new theoretical and practical basis for preventing hepatic IR injury, with the aim of improving the success rate of liver transplantation and reducing postoperative rejection.

[1]Organ Transplantation Center, The Institute of Transplantation Science, The Affiliated Hospital of Qingdao University, Qingdao, Shandong Province, China
[2]Lead contact
*Correspondence: caijinzhen@qdu.edu.cn
https://doi.org/10.1016/j.isci.2024.110280

RESULTS

Proto-oncogene serine/threonine-protein kinase was induced in hypoxia–reoxygenation MIHA cells and a mouse model of hepatic ischemia-reperfusion injury

To investigate the expression level of Pim-1 in hepatic IR, we established a hypoxia–reoxygenation (HR) model of MIHA cells *in vitro*. The results of western blot (WB) and quantitative polymerase chain reaction (qPCR) showed that after the cells were reoxygenated for 2, 6, and 12 h, Pim-1 levels gradually increased with reoxygenation time (Figures 1A and 1B). Moreover, to further determine the correlation between Pim-1 and ischemia−reperfusion, we established a mouse hepatic ischemia−reperfusion model by randomly dividing the mice into ischemia−reperfusion and sham groups. In the ischemia−reperfusion group, mice were euthanized at 0, 6, 12, and 24 h of reperfusion after ischemia. Histological assessment of hepatic injury was performed using hematoxylin and eosin (H&E) staining, and necrosis was observed in the ischemia−reperfusion group at 6, 12 and 24 h after reperfusion (Figure 1C). We also found that messenger RNA (mRNA) and protein levels of Pim-1 after 6, 12, and 24 h of reperfusion in the ischemia−reperfusion group were higher than those in the sham group (Figures 1D and 1E). Immunohistochemical staining also revealed that the expression of Pim-1 increased with increasing reperfusion time (Figure 1F). These data suggest that Pim-1 was upregulated in hypoxia–reoxygenation MIHA cells and a mouse model of liver IR.

Proto-oncogene serine/threonine-protein kinase was upregulated in reperfused liver tissues of patients with liver transplantation

To study the correlation between Pim-1 expression and human liver IR, we collected liver samples from 20 patients before and after reperfusion during liver transplantation operation and serum samples 12 h after surgery. qPCR analysis showed that the mRNA expression of Pim-1 in liver tissues was significantly upregulated in hepatic IR after reperfusion (Figures 2A and 2B). Furthermore, Western blot analysis showed that the protein expression level of Pim-1 was consistent with the mRNA expression level (Figure 2C). To further validate the results of *in vivo mouse* experiments, we stained Pim-1 in liver tissues before and after transplant reperfusion using immunohistochemical techniques. The results showed that Pim-1 staining increased during ischemia−reperfusion (Figure 2D). To evaluate the effect of Pim-1 on liver IR injury, we measured the serum levels of alanine aminotransferase (ALT) and aspartate aminotransferase (AST) using an automated chemistry analyzer, and the results showed that Pim-1 was negatively correlated with the expression of ALT and AST (Figures 2E and 2F), indicating that Pim-1 has a protective effect on liver IR. In addition, we further collected clinical data from 50 patients and divided them into two groups based on the levels of PIM-1 for analysis to verify the recovery of postoperative liver function damage. The results showed that the high PIM-1 group had a reduced incidence of EAD (12% vs. 28%; $p = 0.005$) and postoperative hospitalization (19 [IQR:16–26] vs. 34 [IQR:22–65] days, $p = 0.024$) days compared to the low PIM-1 group. Therefore, high levels of PIM-1 are correlated with improving postoperative liver function recovery in patients after liver transplantation.

Proto-oncogene serine/threonine-protein kinase expression inhibits hepatocyte apoptosis during hypoxia–reoxygenation

During hepatic IR, a series of pathophysiological processes can lead to cell apoptosis. To evaluate the effect of Pim-1 on hepatocyte apoptosis during HR, we used small interfering RNA (siRNA) and lentivirus overexpression to construct Pim-1 knockdown (siPim-1) and overexpression (Pim-1) cell lines in MIHA cells. First, the MIHA cells overexpressing and knocking down Pim-1 were verified at the mRNA level. The PCR results showed that the construction of MIHA cell models with Pim-1 overexpression and knockdown was successful (Figures 3A and 3D). Then, MIHA cells with low and overexpression of Pim-1 were treated with hypoxia and reoxygenation for 12 h. We detected the expression of Pim-1 and apoptosis-related proteins, including caspase 3, B-cell lymphoma-2 (Bcl-2), and Bcl2-associated X protein (Bax), in the cells. Western blot analysis showed that the overexpression of Pim-1 significantly reduced the levels of activated caspase 3 and Bax and upregulated the level of Bcl2 (Figure 3B). In contrast, the levels of activated caspase 3 and Bax were significantly increased, and the level of Bcl2 was decreased in the siPim-1 group after HR (Figure 3E), indicating that the protective effect of Pim-1 had disappeared. To further verify the impact of Pim-1 on apoptosis, we detected the apoptosis of MIHA cells overexpressing Pim-1 and with Pim-1 knockdown using a terminal deoxynucleotidyl transferase biotin-dUTP nick end labeling (TUNEL) kit. The results showed that HR treatment after the overexpression of Pim-1 significantly decreased the apoptosis ratio of cells (Figure 3C). In contrast, HR treatment after interference with Pim-1 significantly increased the proportion of apoptotic cells (Figure 3F). Using ectopically overexpression of Pim-1 to rescue Pim-1 from siRNA depletion reduced the proportion of apoptotic cells (Figure 3F). These data indicate that Pim-1 can inhibit hepatocyte apoptosis and play an important protective role during hepatic IR.

Inhibition of proto-oncogene serine/threonine-protein kinase aggravated liver ischemia-reperfusion injury *in vivo*

To investigate the roles of Pim-1 in hepatic IR, we intraperitoneally injected mice with TCS Pim-1, an effective, selective, and ATP-competitive Pim-1 kinase inhibitor, to establish a mouse model with low Pim-1 expression. The dosage of TCS was 5 mg/kg based on previous studies. Immunohistochemical results showed that the expression of Pim-1 in the liver tissue of mice was significantly decreased after the application of TCS Pim-1 (Figure 4A). Then, TCS Pim-1 and control mice were subjected to hepatic IR, and damaged liver tissues were harvested for histopathologic analysis. H&E staining showed that the inhibition of Pim-1 resulted in markedly higher necrotic rates (Figure 4B). In addition, Ki67 immunohistochemical staining (Figure 4C) and TUNEL (Figure 4D) were used to evaluate the effects of Pim-1 inhibition on hepatocyte proliferation and apoptosis during liver IR. The results showed that compared with the control group, the inhibition of Pim-1 reduced the

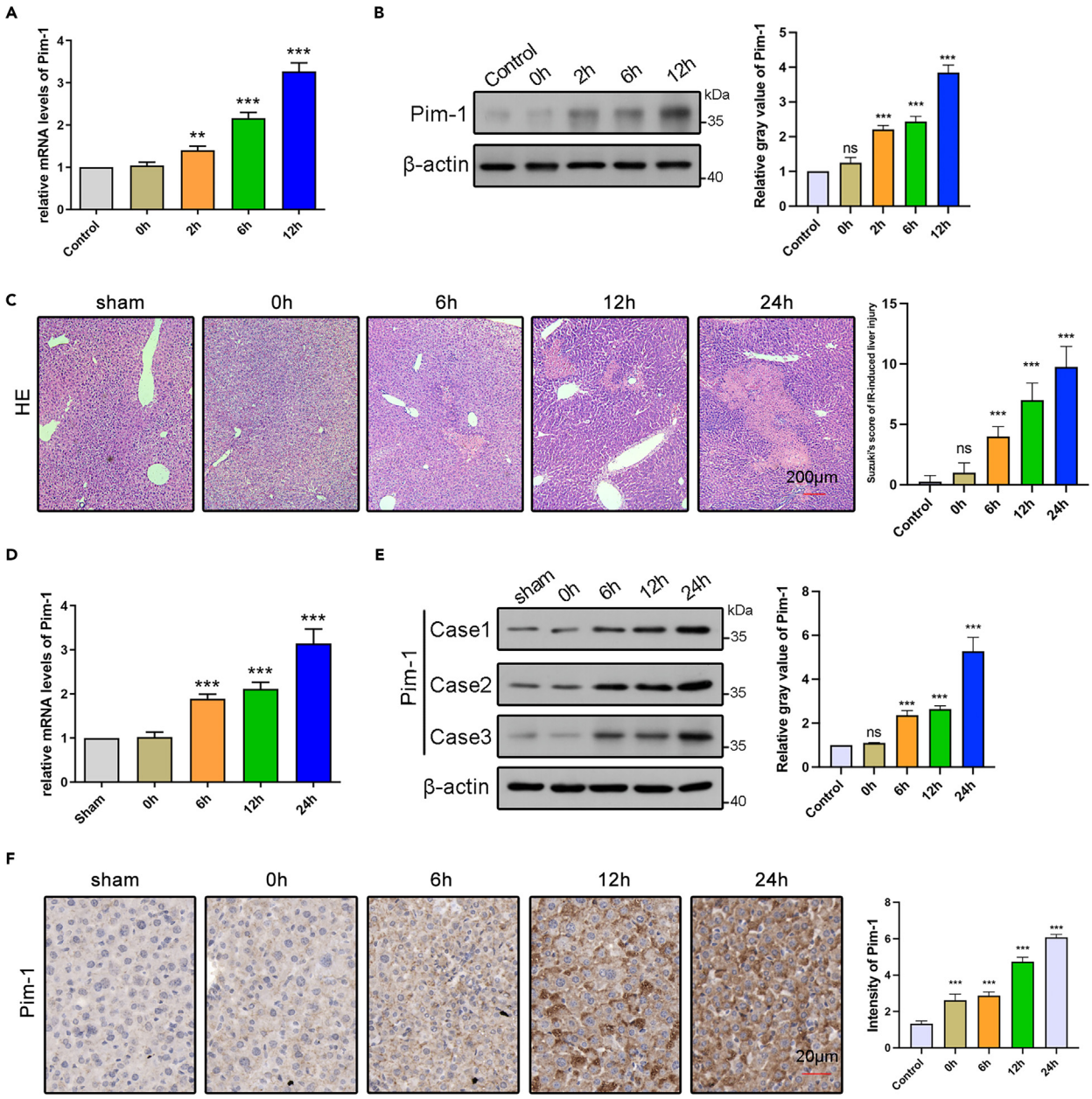

Figure 1. Pim-1 was upregulated in hypoxia–reoxygenation MIHA cells and a mouse model of hepatic ischemia–reperfusion

(A) Quantitative PCR and (B) western blot analyses of Pim-1 in MIHA cells subjected to control conditions or hypoxia–reoxygenation challenge for the indicated periods (0, 2, 6, and 12 h; $n = 3$ for each group). $^{**}p < 0.01$, $^{***}p < 0.001$, vs. control.

(C) Representative H&E staining of liver sections in the sham-operated and ischemia–reperfusion groups at the indicated periods postreperfusion (0, 6, 12, 24 h). Scale bar, 200 μm $^{***}p < 0.001$, vs. sham.

(D) mRNA and (E) protein levels of Pim-1 in the livers of mice subjected to sham treatment or ischemia for 1 h followed by reperfusion for the indicated periods (0, 6, 12, and 24, mice $n = 5$ for each group). $^{***}p < 0.001$, vs. sham.

(F) Representative immunohistochemical staining of Pim-1 in the sham and ischemia–reperfusion groups at the indicated periods postreperfusion (0, 6, 12, and 24 h). Scale bar, 50 μm $^{***}p < 0.001$, vs. sham. Student's t test was used. All data are presented as the means ± SDs. mRNA, messenger RNA; H&E, hematoxylin and eosin; sham, sham-operated.

expression of Ki67 and increased cell apoptosis under hepatic IR stimulation. Levels of serum ALT and AST were also increased in the IR + TCS Pim-1 group compared with those in the ischemia–reperfusion group (Figures 4E and 4F). These data suggest that the inhibition of Pim-1 might contribute to the susceptibility of livers to IR injury *in vivo*.

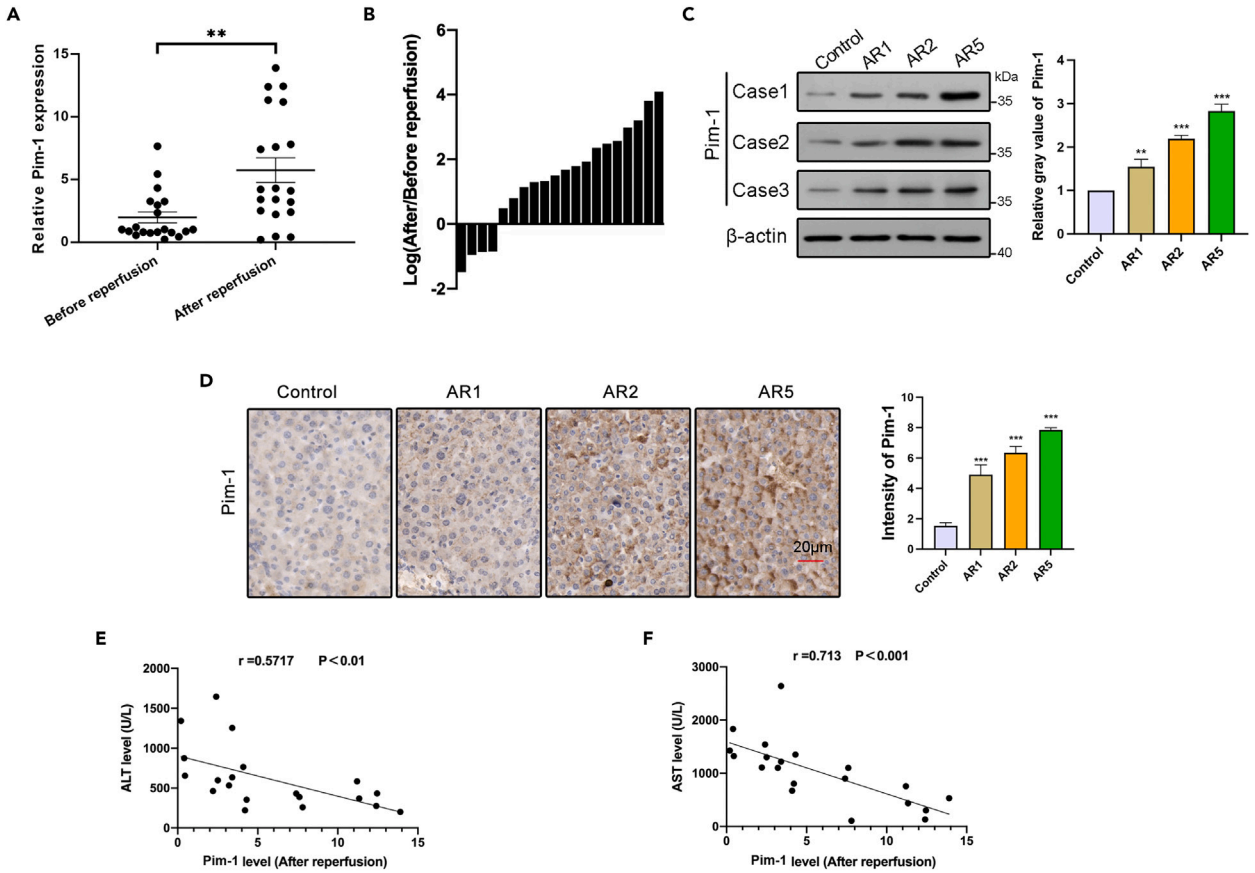

Figure 2. Pim-1 was increased in reperfused liver samples of patients with liver transplantation

(A) Quantitative PCR analysis of Pim-1 in the samples of patients with liver transplantations before and after reperfusion ($n = 20$). $^{**}p < 0.01$. Student's t test was used.

(B) The bars represent the relative Pim-1 expression with the ratios of its levels in liver tissues after versus before reperfusion (logarithmic scale).

(C) Western blot analysis of Pim-1 in the samples of patients with liver transplantation before and after reperfusion (AR) for the indicated periods (1, 2, and 5 h, $n = 5$). The data were normalized to the expression levels of β-actin. $^{**}p < 0.01$, $^{***}p < 0.001$. Student's t test was used.

(D) Immunohistochemistry detected the expression of Pim-1 before (control) and after reperfusion for the indicated periods (1, 2, and 5 h). Scale bar, 50 μm $^{***}p < 0.001$. Student's t test was used.

(E) The correlation between Pim-1 mRNA levels in liver tissues after reperfusion and serum ALT levels was analyzed ($n = 20$). Pearson analysis was used.

(F) The correlation between Pim-1 levels in liver tissues after reperfusion and serum AST levels was analyzed ($n = 20$). Pearson analysis was used. All data are presented as the means ± SDs. mRNA, messenger RNA, AR, after reperfusion; ALT, alanine aminotransferase; AST, aspartate aminotransferase.

Proto-oncogene serine/threonine-protein kinase kinase upregulates *p*-dynamics-related protein 1 and inhibits dynamics-related protein 1 translation to the mitochondria during hepatic ischemia-reperfusion

It was shown that Pim-1 inhibits the mitochondrial translocation of Drp1 during myocardial ischemia, resulting in reduced mitochondrial division. To investigate whether Pim-1 has the same function in hepatic IR, we detected the expression of Pim-1, total Drp1 (T-Drp1), and phosphorylated Drp1 (P-Drp1 Ser637) in siPim-1 and control cells under normoxia and HR. The results showed that compared with the control group under normoxia, the expression of Pim-1 and P-Drp1 Ser637 increased in the HR group (Figure 5A). Importantly, compared with the control group under normoxia, the expression of Pim-1 and P-Drp1 Ser637 in the HR-siPim-1 group decreased (Figure 5A), and the content of DRP1 in mitochondria increased (Figure 5B). Moreover, the expression of other fission factors, including MFF and FISI, did not change (Figure 5A). To further verify the above results, we detected the expression of T-Drp1 and P-Drp1 Ser637 in the liver tissues of control and TCS Pim-1 mice under IR using immunohistochemistry (Figure 5C). Moreover, we performed the double-stained immunofluorescence with antibodies against Drp1 and MitoTracker (Figure 5D). The results showed that compared with the control group under IR, the staining intensity of P-Drp1 Ser637 and MitoTracker was decreased after inhibiting Pim-1, and the total Drp1 expression did not change significantly. Furthermore, we extracted the mitochondria from the above mouse hepatocytes and detected the expression of Drp1 in the mitochondria using Western blotting, and the results were consistent with those described above (Figure 5E). Taken together, the results showed that Pim-1 can also regulate the phosphorylation of Drp1 and inhibit Drp1 translation to the mitochondria during liver IR.

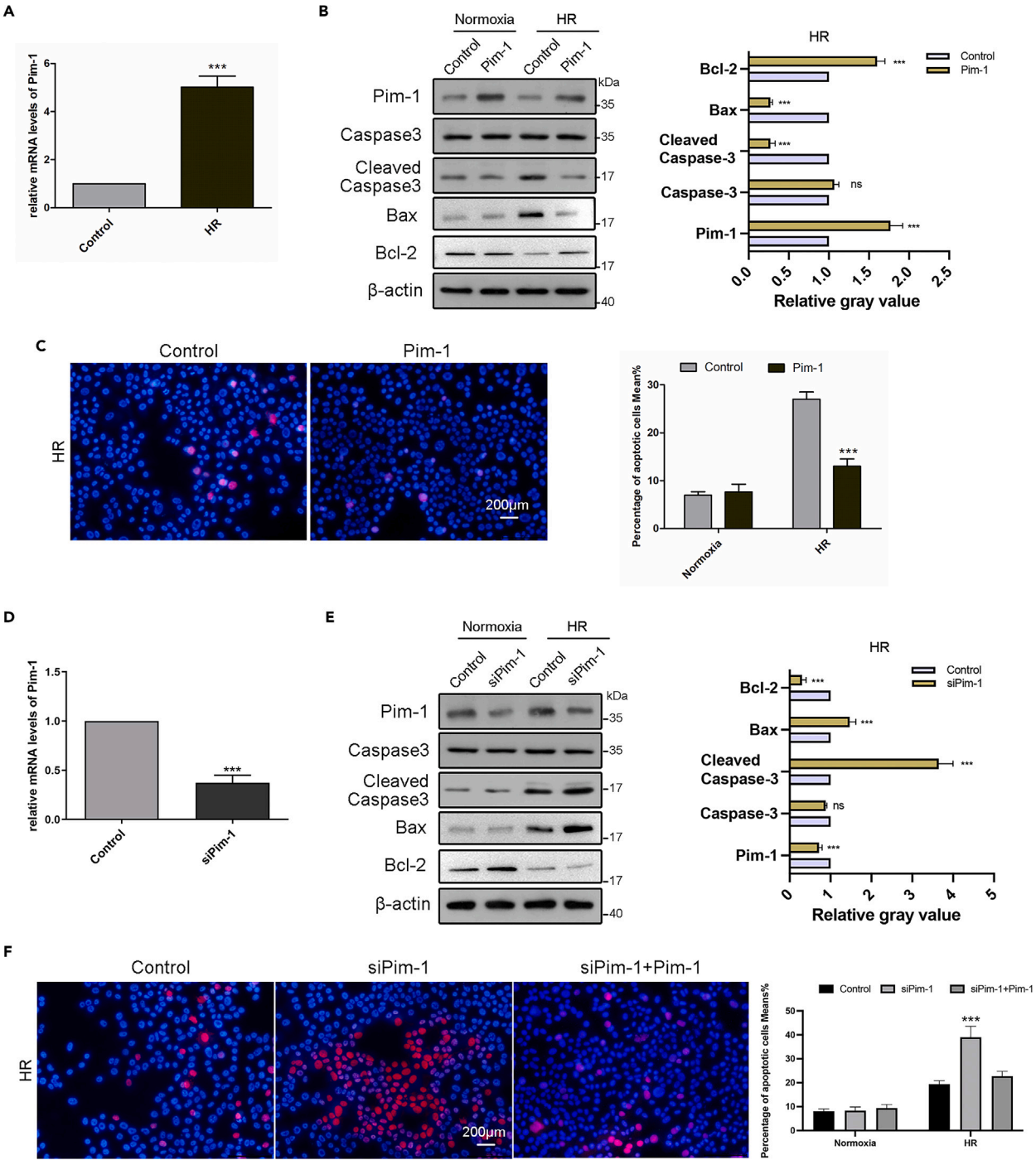

Figure 3. The effect of Pim-1 on cell apoptosis under HR stimulation

(A) Quantitative PCR analysis of Pim-1 in MIHA cells subjected to control conditions or hypoxia–reoxygenation (HR) challenge 12 h postreperfusion (n = 3). ***p < 0.001. Student's t test was used.

(B) Western blot analysis of Pim-1, caspase 3, cleaved caspase 3, Bax and Bcl-2 proteins in MIHA cells stably overexpressing Pim-1 and their control cells under normoxia or HR challenge 12 h postreperfusion (n = 3). β-Actin was used as a loading control. ***p < 0.001. Student's t test was used. The data were normalized to the expression levels of β-actin.

(C) Representative images from a TUNEL assay and the proportions of apoptosis in MIHA cells stably overexpressing Pim-1 and their control cells under normoxia or hypoxia–reoxygenation challenge 12 h postreperfusion (n = 3). ***p < 0.001 vs. control. Student's t test was used.

Figure 3. *Continued*

(D) Quantitative PCR analysis of Pim-1 in MIHA cells with Pim-1 knockdown and control cells under normoxia or HR challenge at 12 h postreperfusion ($n = 3$). ***$p < 0.001$. Student's t test was used.

(E) Western blot analysis of Pim-1, caspase 3, cleaved caspase 3, Bax and Bcl-2 proteins in MIHA cells with Pim-1 knockdown and control cells under normoxia or hypoxia–reoxygenation challenge 12 h postreperfusion ($n = 3$). β-Actin was used as a loading control. ***$p < 0.001$. Student's t test was used. The data were normalized to the expression levels of β-actin.

(F) Representative images of a TUNEL assay and the proportions of apoptosis in MIHA cells with Pim-1 knockdown, control cells, and ectopically overexpression of Pim-1 from Pim-1 knockdown under normoxia or hypoxia–reoxygenation challenge 12 h postreperfusion ($n = 3$). ***$p < 0.001$ vs. control. Student's t test was used. All data are presented as the means ± SDs. HR, hypoxia–reoxygenation.

Proto-oncogene serine/threonine-protein kinase maintains mitochondrial morphological integrity

The above results show that the upregulation of Pim-1 during hepatic IR can inhibit the mitochondrial translocation of Drp1, which raises the question as to whether it affects the morphology of mitochondria. Mitochondrial electron microscopy results confirmed that electron-dense mitochondrial cristae and clear membranes could be observed in liver tissue sections from sham group mice and MIHA cells under normoxia (Figures 6A and 6G). However, the mitochondrial volumes in hepatocytes of mice in the IR group and MIHA cells in the HR group were increased unevenly, with obvious swelling, and presented globular or irregular outlines, as well as significantly increased numbers of autophagic vesicles compared with the sham and normoxia groups (Figures 6B and 6H). Importantly, these morphological changes observed in the IR and HR groups were diffused in the Pim-1 low expression group, which exhibited a greater number of autophagic vacuoles and serious damage to the mitochondria (Figures 6C and 6I). In addition, low expression of Pim-1 increased the length, area, and perimeter of mitochondria, all of which suggest aggravated mitochondrial injury *in vivo* and *in vitro* during IR or HR (Figures 6D–6F, and 6J–6L). Mitochondrial fragmentation releases cytochrome *c* into the cytosol, which initiates caspase activation. We further tested the levels of cytochrome *c* in the cytoplasm and mitochondria of MIHA cells under HR. The protein expression of cytochrome *c* was increased in the cytosol and decreased in the mitochondria in the siPim-1+HR group compared with the HR and normoxia groups. Hence, Pim-1 plays an important role in protecting mitochondrial morphological integrity.

Elevated proto-oncogene serine/threonine-protein kinase expression is dependent on H3K9me3 during liver ischemia-reperfusion

The molecular mechanisms of Pim-1 upregulation during liver IR are unclear. We therefore wondered whether the level of Pim-1 expression might be dependent on an epigenetic mechanism. Previous studies have found that the trimethylation of lysine 9 on histone H3 (H3K9me3) can activate the expression of Pim-1 in liver cancer cells to accelerate the progression of liver cancer.[18] Hence, we hypothesized that histone methylation may be a regulatory mechanism of Pim-1 upregulation in HR. To verify this hypothesis, we detected the expression level of H3K9me3 in hepatocytes, and WB results showed that the expression of H3K9me3 in HR-MIHA cells was significantly higher than that in normal MIHA cells (Figure 7A). Then, to detect the binding between H3K9me3 and the Pim-1 promoter, we constructed three Pim-1 gene promoter sequences of different lengths (205 bp, 189 bp, 198 bp) for a chromatin immunoprecipitation (ChIP) experiment. The results of qPCR using primers specific for the Pim-1 promoter showed that compared with the control group, the binding of H3K9me3 and the Pim-1 promoter was increased in the HR group (Figure 7B), which indicated that H3K9me3 could indeed bind to the promoter sequence of Pim-1. To further verify the effect of H3K9me on Pim-1 expression, we treated MIHA cells with chaetocin, an inhibitor of H3K9me3, using a dosage of 30 nM based on previous studies. Both Western blot and qPCR results showed that chaetocin inhibited the expression of H3K9me3 as well as Pim-1 in MIHA cells (Figures 7C and 7D). Next, we constructed a pGL3 fluorescent reporter plasmid with expression driven by the Pim-1 promoter and transfected it into MIHA cells. The relative luciferase activity of the Pim-1 promoter in the HR group was significantly higher than that in the control group, while the luciferase activity of the Pim-1 promoter in the HR plus chaetocin inhibitor group was significantly lower than that in the control group (Figure 7E). The above results suggest that H3K9me3 transactivates the expression of Pim-1. Together, these results indicate that hypoxia-mediated aberrant H3K9me3 levels activated the expression of Pim-1.

DISCUSSION

This study showed that H3K9me3 can transactivate the expression of Pim-1 during hepatic IR, and the overexpression of Pim-1 can inhibit the dephosphorylation of the Drp1 Ser637 site, inhibit the transfer of Drp1 to the outer membrane of mitochondria, stabilize the mitochondrial membrane, alleviate the excessive mitosis and apoptosis mediated by hypoxia–reoxygenation, and improve hepatocyte injury during hepatic IR. Therefore, Pim-1 may become a new target for the development of therapeutic strategies for hepatic IR.

In recent years, an increasing number of studies on liver IR have been published.[12] Although efforts have been made to explore the mechanism and preventive strategies of IR injury in clinical practice, hepatic IR is still a serious postoperative complication that increases the possibility of postoperative morbidity, mortality, and graft failure.[19,20] Ischemia–reperfusion injury can be divided into two types: "warm" ischemia–reperfusion injury and "cold" ischemia–reperfusion injury.[21–23] Warm ischemia–reperfusion injury triggered by hepatocyte injury occurs during liver transplantation surgery or during various forms of shock or trauma and may lead to liver and even multiple organ failure.[22] Cold ischemia–reperfusion injury caused by hepatic sinusoidal endothelial cell injury and microcirculation damage occurs in the process of

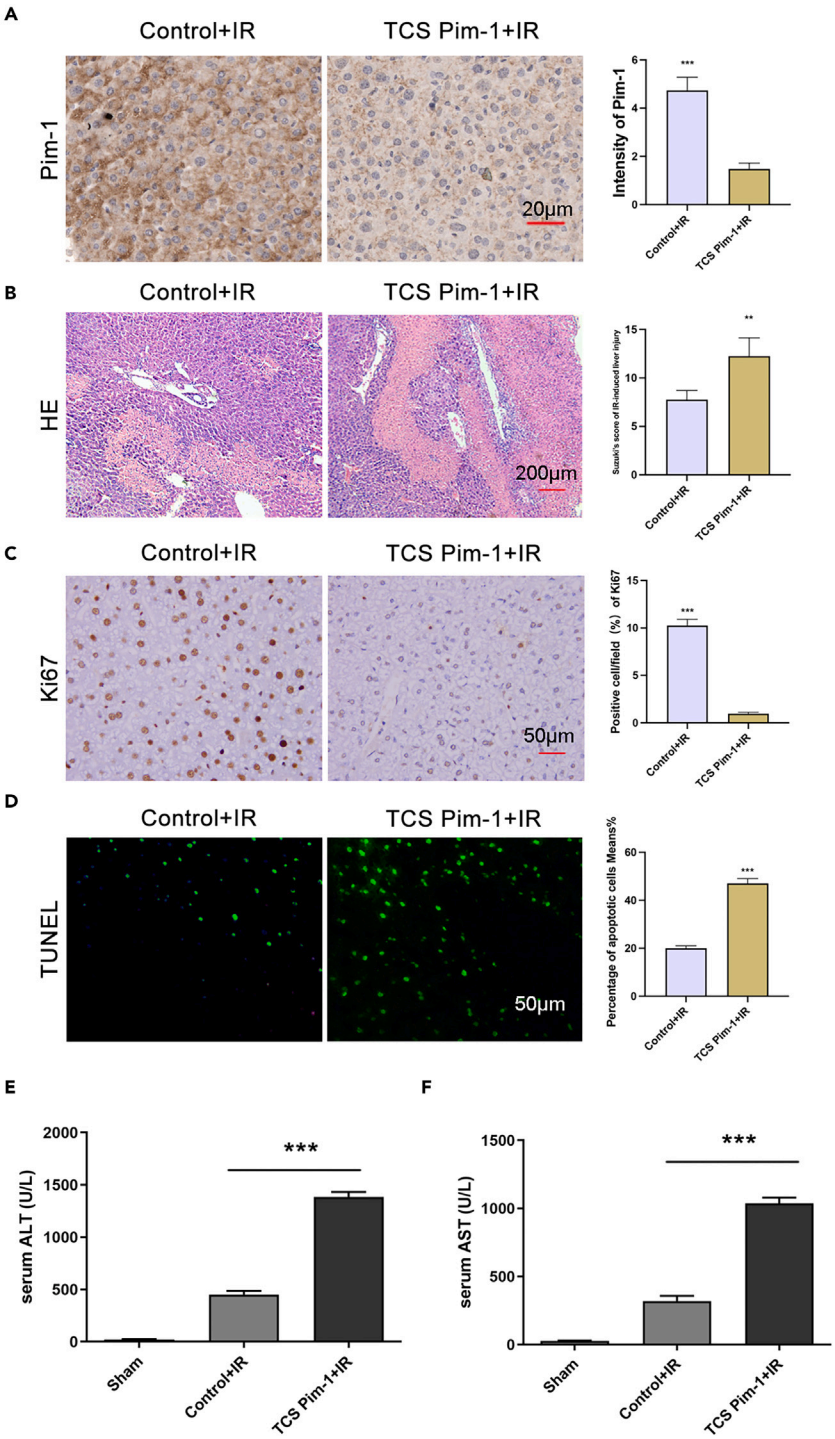

Figure 4. The effect of Pim-1 inhibition on IR reduced liver damage

Mice were intraperitoneally injected with a Pim-1 kinase inhibitor (TCS Pim-1, 5 mg/kg) for 5 days to decrease Pim-1 expression. Then, mice with inhibited Pim-1 and controls were used to establish a mouse hepatic IR model.

(A) Immunohistochemical staining showing the expression levels of Pim-1 in liver lobes of the TCS-Pim-1 and control groups after IR injury (12 h postreperfusion, $n = 5$ per group). ***$p < 0.001$ vs. control+IR group. Student's t test was used. Scale bar, 50 μm.

(B) H&E staining of liver sections was observed in the TCS-Pim-1 and control groups after IR injury (12 h postreperfusion, $n = 5$ per group). **$p < 0.01$ vs. control+IR group. Student's t test was used. Scale bar, 200 μm.

Figure 4. *Continued*

(C) Immunohistochemical staining showing the expression levels of Ki67 in liver lobes of the TCS-Pim-1 and control groups after IR injury (12 h postreperfusion, $n = 5$ per group). ***$p < 0.001$ vs. control+IR group. Student's t test was used. Scale bar, 50 μm.

(D) TUNEL staining of liver lobes of the TCS-Pim-1 group and control group after IR injury (12 h postreperfusion, $n = 5$ per group). ***$p < 0.001$ vs. control+IR group. Student's t test was used.

(E and F) Serum ALT and AST were measured by an automated chemistry analyzer. Serum ALT (E) and AST (F) levels in sham, IR + control and IR + TCS Pim-1 mice 12 h postreperfusion. ***$p < 0.001$. The Mann–Whitney U test was used. All data are presented as the means ± SDs. TSC, an ATP-competitive Pim-1 kinase inhibitor; IR, ischemia–reperfusion; ALT, alanine aminotransferase; AST, aspartate aminotransferase; sham, sham-operated.

in vitro preservation and is usually accompanied by warm ischemia–reperfusion injury during liver transplantation surgery.[24] Although the initial target cells of these two types of ischemia–reperfusion injury may be different, they share a common mechanism in disease etiology, namely, cell death.

As a protein serine threonine kinase, Pim-1 exists in the cytoplasm and nucleus and has a wide range of biological functions,[25,26] such as apoptosis inhibition,[27] cell cycle regulation,[28] cell metabolic activity,[29] and stable mitochondrial integrity.[30] Studies have shown that Pim-1 is highly expressed in cardiac progenitor cells, which can promote cell cycle progression and mitosis and is one of the important mechanisms of repair after myocardial infarction.[31] The expression and activity of Pim-1 in the blood system and solid tumor cells are regulated by apoptosis-related signaling pathways and cooperate with other apoptotic factors to participate in apoptosis inhibition.[32] One of the main anti-apoptosis mechanisms of Pim-1 is the regulation of the activity of apoptotic proteins such as Bcl-2 and Bad,[33] which can be inactivated by phosphorylating the serine residues at positions 112 and 136 of Bad, and Pim-1 can also participate in apoptosis inhibition by regulating other apoptosis suppressors.[34] Borillo et al.[35] found that when cardiomyocytes were injured by chemical reperfusion injury, Pim-1 migrated to mitochondria, the release of cytochrome *c* (Cyt c) was inhibited, and the stability of mitochondria was maintained. Recently, the inhibitory effect of Pim-1 on apoptosis has become a focus of research efforts, but there have been no reports on hepatic IR. Therefore, we studied the role of Pim-1 in liver IR for the first time. First, we detected the expression of Pim-1 in the process of hepatic IR and found that the expression of Pim-1 at the mRNA and protein levels increased significantly in an HR-stimulated MIHA cell model, a surgery-induced hepatic IR animal model, and patient liver transplantation samples and gradually increased with time, suggesting that Pim-1 may be a key regulatory molecule in regulating IR injury. We also found that the expression of Pim-1 in the liver tissue of patients with liver transplantations was negatively correlated with the levels of ALT and AST in serum. Serum ALT and AST are markers of liver injury, suggesting that Pim-1 is involved in hepatic IR. As mentioned above, Pim-1 participates in apoptosis inhibition in solid tumors and hematological cancers in collaboration with other apoptosis factors. It has a pro-cancer effect. In the application of PIM-1, we only need to monitor the expression of downstream genes and the activation of oncogenes in real time and make corresponding drug withdrawal treatment in time. PIM-1 still has high clinical application value in improving liver IRI.

Under physiological conditions, mitochondrial fission and fusion are in a state of dynamic equilibrium to maintain mitochondrial homeostasis.[36] In hepatic IR, persistent metabolic stress can lead to the overexpression of the mitochondrial fission-related proteins DRP-1 and FIS-1, which can lead to mitochondrial fragmentation and trigger apoptosis.[9,37] The Drp1 protein is a conserved GTPase and a key protein regulating mitochondrial fission.[38] It is mainly located in the cytoplasm and binds to the outer mitochondrial membrane. It can translocate to the outer mitochondrial membrane to mediate mitochondrial fission through postexpression modifications, including phosphorylation, nitrosylation, sumoylation, and ubiquitination, among which the dephosphorylation of the Drp1 Ser637 site is an important modification method to promote Drp1 translocation to mitochondria.[39] Studies have shown that ischemia–reperfusion can cause the dephosphorylation of the Drp1 Ser637 site and promote the transfer of Drp1 to the mitochondrial outer membrane.[40,41] After a large amount of Drp1 is transferred to the outer mitochondrial membrane, the mitochondria are damaged, and the mitochondrial cristae are also destroyed. Previous studies have shown that the Cyt *c* stored in the mitochondrial matrix is released, which activates the downstream caspase enzyme and leads to apoptosis.[18,39] Our results are consistent with these previous findings; i.e., the phosphorylation level of Drp1 Ser637 in Pim-1 knockdown MIHA cells decreased after hypoxia and reoxygenation, the level of Drp1 Ser637 phosphorylation in MIHA cells decreased, the expression of the apoptotic protein cleaved caspase 3 increased, and the content of Drp1 in mitochondria increased. The mouse model with reduced Pim-1 further confirmed that Pim-1 regulates the phosphorylation of Drp1 and inhibits the mitochondrial translocation of Drp1. At the same time, we observed vascular degeneration and mitochondrial cristae damage in mitochondria in mouse hepatocytes using electron microscopy. The above results indicate that Pim-1 in hepatic IR leads to an imbalance of mitochondrial fission and fusion by downregulating the phosphorylation level of Drp1 Ser637, thus mediating induced apoptosis.

H3k9me3 can transactivate the expression of Pim-1, and previous studies have shown that H3k9me3 can induce the expression of Pim-1 to accelerate the progression of liver cancer cells.[42] In this study, we detected the interaction between H3k9me3 and Pim-1 through a ChIP experiment and a luciferase activity assay. H3k9me3 bound to the promoter of Pim-1, and when an inhibitor of H3k9me3 was added, it significantly inhibited Pim-1-dependent transcriptional activity. Therefore, we believe that the transcriptional activity of Pim-1 is regulated by H3k9me3 in hepatic IR.

In conclusion, we used clinical specimens from patients with liver transplantation, a mouse liver ischemia–reperfusion model, and a hypoxia–reoxygenation-MIHA cell model to study the role of Pim-1 in hepatic IR. The mechanism by which Pim-1 protects the liver from IR injury is shown in graphical abstract. Our results provide support for a new approach for studying the role of Pim-1 in liver IR and for the potential clinical application of Pim-1 in improving hepatic IR injury.

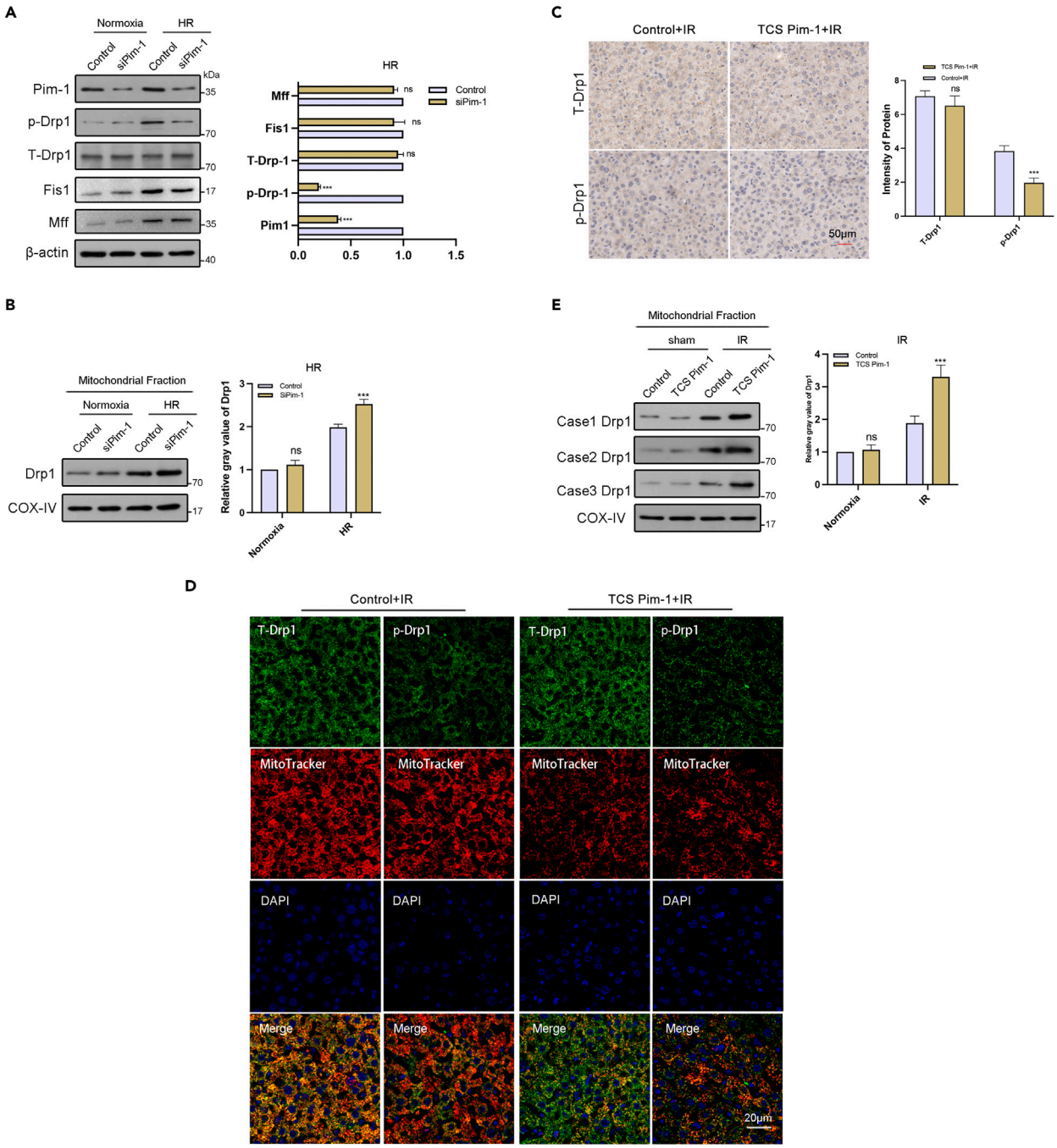

Figure 5. Pim-1 kinase targets Drp1 and affects Drp1 translation to the mitochondria

(A) Western blot analysis of Pim-1, *p*-Drp1 Ser637, T-Drp1, Fis1, and Mff proteins in siPim-1 MIHA cells and their control cells under normoxia or HR 12 h postreperfusion ($n = 3$ per group). β-Actin was used as a loading control. ***$p < 0.001$. Student's t test was used.

(B) Western blot analysis of Drp1 proteins in the mitochondria of siPim-1 MIHA cells and their control cells with the indicated stimulation ($n = 3$ per group). COX-IV was used as a loading control. ***$p < 0.001$. Student's t test was used.

(C) Representative images and quantification of total Drp1 (T-Drp1) and *p*-Drp1 Ser637 immumohistochemical staining in liver lobes of TCS Pim-1 and control mice under IR ($n = 5$ per group). Scale bar, 50 μm ***$p < 0.001$. Student's t test was used.

(D) Representative images of total Drp1, *p*-Drp1 Ser637, and MitoTracker immunofluorescence staining in liver lobes of TCS Pim-1 and control mice under IR ($n = 5$ per group). Scale bar, 50 μm.

(E) Western blot analysis of DRP1 proteins in the mitochondria of TCS Pim-1 and control mice under IR ($n = 5$ per group). ***$p < 0.001$. Student's t test was used. All data are presented as the means ± SDs. HR, hypoxia–reoxygenation; SiPim-1, small interfering RNA targeting Pim-1; IR, ischemia–reperfusion.

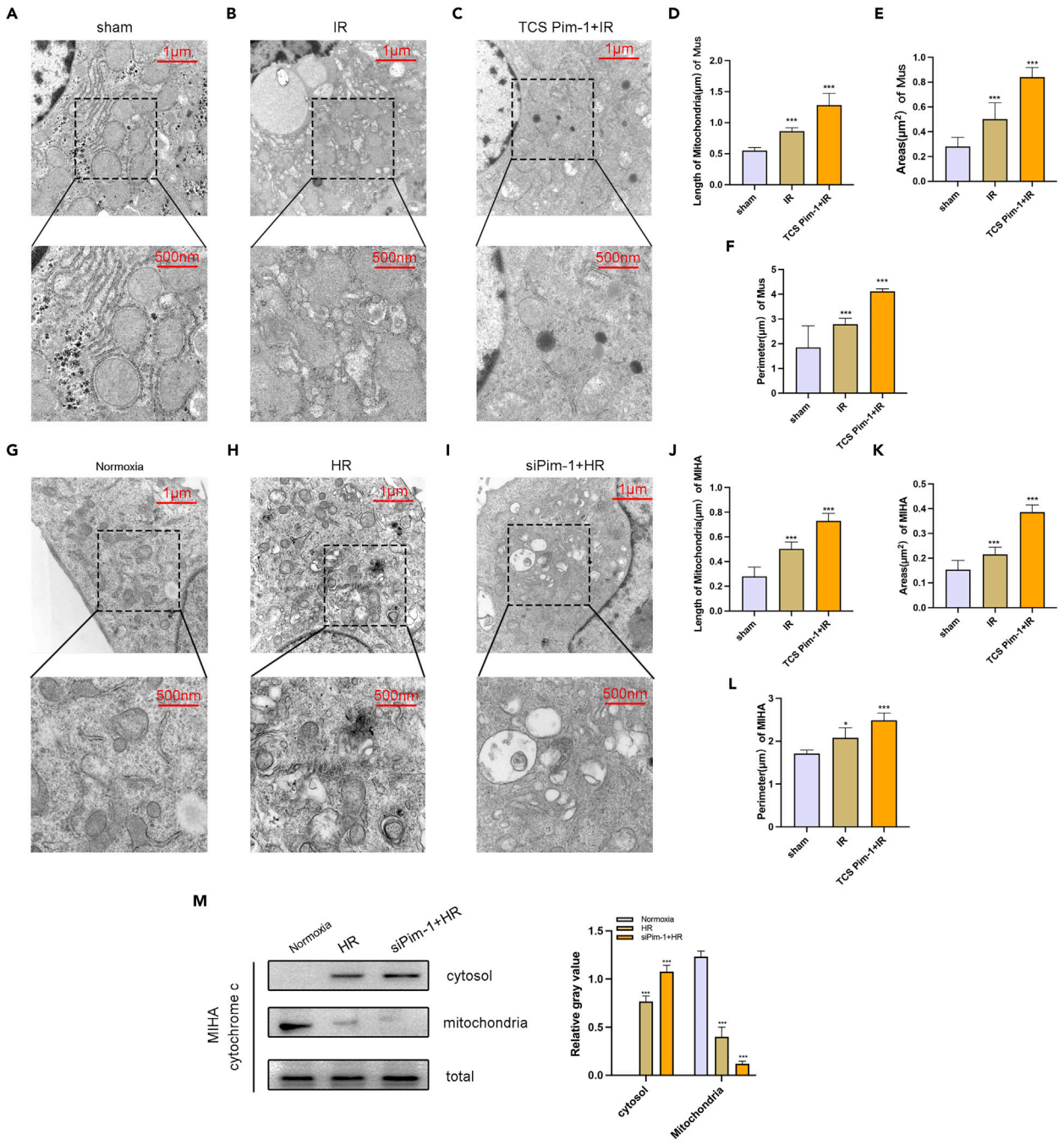

Figure 6. Pim-1 maintains mitochondrial morphological integrity

Transmission electron microscopy was used to measure mitochondrial morphology in the liver tissue of mice and MIHA cells.

(A–C) Representative images and morphometric analysis of liver tissue in the sham operation group (A), IR group (B) and TCS Pim-1+IR group (C). Scale (top) = 1 μm, scale (bottom) = 500 nm.

(D–F) Mitochondrial morphology was quantified using Fiji/ImageJ. Comparison of mitochondrial length (D), area (E), and perimeter (F) in liver tissue of mice ($n = 5$ per group). ***$p < 0.001$. Student's t test was used.

(G–I) Representative images of MIHA cells in the normoxia group (G), HR group (H), and siPim-1+HR group (I). Scale (top) = 1 μm, scale (bottom) = 500 nm.

(J–L) Comparison of mitochondrial length (D), area (E), and perimeter (F) in MIHA cells ($n = 3$ per group). ***$p < 0.001$. Student's t test was used. All data are presented as the means ± SDs.

(M) Western blot analysis of cytochrome *c* in the cytoplasm and mitochondria of MIHA cells. ***$p < 0.001$. Student's t test was used. IR, ischemia–reperfusion; HR, hypoxia–reoxygenation; SiPim-1, small interfering RNA targeting Pim-1; Mus, mouse.

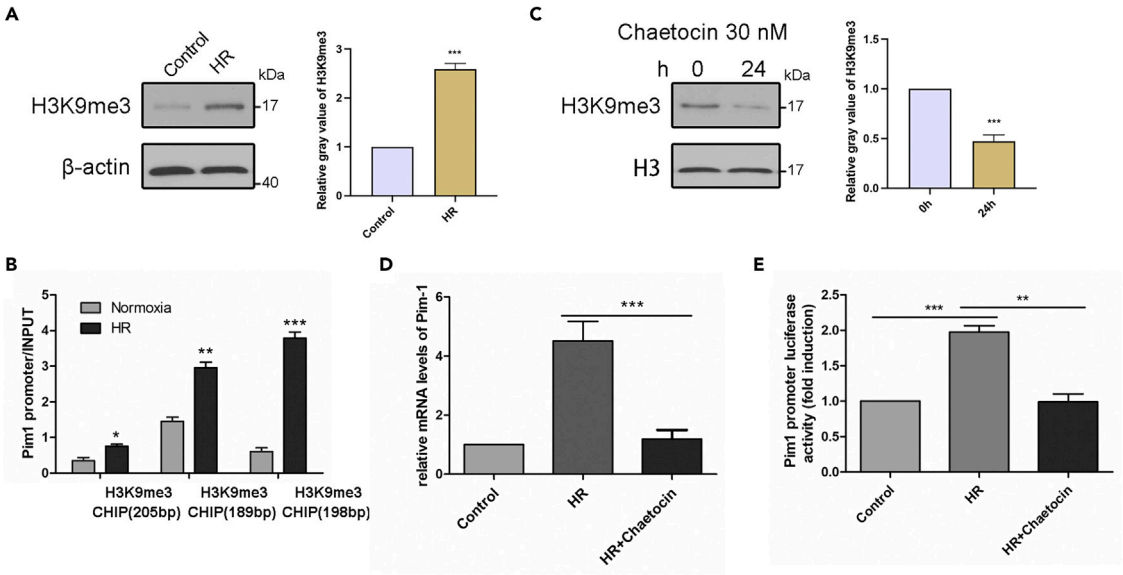

Figure 7. H3K9me3 promotes Pim-1 expression during HR

(A) Western blot analysis of H3K9me3 in MIHA cells subjected to control conditions or HR challenge 12 h postreperfusion ($n = 3$ per group). ***$p < 0.001$. Student's t test was used.

(B) ChIP–qPCR analysis of H3K9me3 binding to the Pim-1 promoter in MIHA cells with the indicated stimulation. Precipitated DNA was quantified with qPCR for promoter regions of the Pim-1 gene ($n = 3$ per group). *$p < 0.05$, **$p < 0.01$, ***$p < 0.001$. Student's t test was used.

(C) Global levels of H3K9me3 by western blot analysis in MIHA cells following chaetocin treatment (30 nM, $n = 3$). ***$p < 0.001$. Student's t test was used.

(D) Pim-1 mRNA levels in MIHA cells under control conditions, HR, or HR plus chaetocin treatment ($n = 3$). ***$p < 0.001$. Student's t test was used.

(E) Pim-1 promoter luciferase activity assay in MIHA cells under control conditions, HR, or HR plus chaetocin treatment ($n = 3$). **$p < 0.01$, ***$p < 0.001$. Student's t test was used.

Limitations of the study

Our study's reliance on *in vitro* and mouse models might not fully capture the complexity of human liver ischemia-reperfusion injury, potentially limiting the generalizability of the findings to clinical settings. The relatively small and homogeneous sample size in the clinical component of the study may not adequately represent the broader population, affecting the universality of the results. While focusing on Pim-1 provides valuable insights, the exclusion of other molecular pathways could overlook the multifaceted nature of hepatic IR injury.

STAR★METHODS

Detailed methods are provided in the online version of this paper and include the following:

- KEY RESOURCES TABLE
- RESOURCE AVAILABILITY
  - Lead contact
  - Materials availability
  - Data and code availability
- EXPERIMENTAL MODEL AND STUDY PARTICIPANT DETAILS
  - Clinical specimens
  - Experimental animals
  - Mouse model of hepatic ischemia–reperfusion and drug treatment
  - Cell culture and transfection
  - Hypoxia/reoxygenation (HR) model
  - Western Blot (WB)
  - ALT and AST detection
  - Quantitative reverse transcription polymerase chain reaction (qRT–PCR)
  - Immunohistochemical staining
  - Hematoxylin and eosin (H&E) staining
  - Terminal deoxynucleotidyl transferase dUTP nick end labeling (TUNEL) assay
  - Transmission electron microscopy (TEM)

ACKNOWLEDGMENTS

The authors would like to thank the Organ Transplantation Center and the Key Laboratory of Organ Transplantation of Affiliated Hospital of Qingdao University for their technical support.

Financial Support: This work was supported by the National Natural Science Foundation of China (81900575, 82272973, 82370666); the China Postdoctoral Science Foundation (2020M672003, 2022T150341); Shandong University youth innovation team (2022KJ300); the Science Foundation of Shandong Province (No. ZR2022MH292).

AUTHOR CONTRIBUTIONS

JC and YD designed the study, analyzed results, supervised experiments, and wrote the article. YD, QX, DD, YJ, SS, ZBL, SW, PJ, and PL performed most of the experiments and analyzed results. XL, XW, YZ, FW, TL, XCS, and BW collected clinical samples and supervised clinicopathological data. JC provided reagents and laboratory apparatus.

DECLARATION OF INTERESTS

The authors have declared that no conflict of interest exists.

Received: June 1, 2023
Revised: September 25, 2023
Accepted: June 13, 2024
Published: June 28, 2024

REFERENCES

1. Mendes-Braz, M., Elias-Miró, M., Jiménez-Castro, M.B., Casillas-Ramírez, A., Ramalho, F.S., and Peralta, C. (2012). The current state of knowledge of hepatic ischemia-reperfusion injury based on its study in experimental models. J. Biomed. Biotechnol. *2012*, 298657.
2. Yan, Z.Z., Huang, Y.P., Wang, X., Wang, H.P., Ren, F., Tian, R.F., Cheng, X., Cai, J., Zhang, Y., Zhu, X.Y., et al. (2019). Integrated Omics Reveals Tollip as an Regulator and Therapeutic Target for Hepatic Ischemia-Reperfusion Injury in Mice. Hepatology *70*, 1750–1769.
3. Yang, W., Chen, J., Meng, Y., Chen, Z., and Yang, J. (2018). Novel Targets for Treating Ischemia-Reperfusion Injury in the Liver. Int. J. Mol. Sci. *19*, 1302.
4. Zhao, L., Li, S., Wang, S., Yu, N., and Liu, J. (2015). The effect of mitochondrial calcium uniporter on mitochondrial fission in hippocampus cells ischemia/reperfusion injury. Biochem. Biophys. Res. Commun. *461*, 537–542.
5. Li, Y., and Liu, X. (2018). Novel insights into the role of mitochondrial fusion and fission in cardiomyocyte apoptosis induced by ischemia/reperfusion. J. Cell. Physiol. *233*, 5589–5597.
6. Rana, A.K., and Singh, D. (2018). Targeting glycogen synthase kinase-3 for oxidative stress and neuroinflammation: Opportunities, challenges and future directions for cerebral stroke management. Neuropharmacology *139*, 124–136.
7. Li, N., Qin, S., Xie, L., Qin, T., Yang, Y., Fang, W., and Chen, M.H. (2018). Elevated Serum Potassium Concentration Alleviates Cerebral Ischemia-Reperfusion Injury via Mitochondrial Preservation. Cell. Physiol. Biochem. *48*, 1664–1674.
8. Wei, N., Pu, Y., Yang, Z., Pan, Y., and Liu, L. (2019). Therapeutic effects of melatonin on cerebral ischemia reperfusion injury: Role of Yap-OPA1 signaling pathway and mitochondrial fusion. Biomed. Pharmacother. *110*, 203–212.
9. Toyama, E.Q., Herzig, S., Courchet, J., Lewis, T.L., Jr., Losón, O.C., Hellberg, K., Young, N.P., Chen, H., Polleux, F., Chan, D.C., and Shaw, R.J. (2016). Metabolism. AMP-activated protein kinase mediates mitochondrial fission in response to energy stress. Science *351*, 275–281.
10. Luo, X., Cai, S., Li, Y., Li, G., Cao, Y., Ai, C., Gao, Y., and Li, T. (2020). Drp-1 as Potential Therapeutic Target for Lipopolysaccharide-Induced Vascular Hyperpermeability. Oxid. Med. Cell. Longev. *2020*, 5820245.
11. Wang, Z., Bhattacharya, N., Weaver, M., Petersen, K., Meyer, M., Gapter, L., and Magnuson, N.S. (2001). Pim-1: a serine/threonine kinase with a role in cell survival, proliferation, differentiation and tumorigenesis. J. Vet. Sci. *2*, 167–179.
12. Yang, Y., Song, S., Meng, Q., Wang, L., Li, X., Xie, S., Chen, Y., Jiang, X., Wang, C., Lu, Y., et al. (2020). miR24-2 accelerates progression of liver cancer cells by activating Pim1 through tri-methylation of Histone H3 on the ninth lysine. J. Cell Mol. Med. *24*, 2772–2790.
13. Yang, G., Zhang, X., Weng, X., Liang, P., Dai, X., Zeng, S., Xu, H., Huan, H., Fang, M., Li, Y., et al. (2017). SUV39H1 mediated SIRT1 transrepression contributes to cardiac ischemia-reperfusion injury. Basic Res. Cardiol. *112*, 22.
14. Blanco-Aparicio, C., Collazo, A.M.G., Oyarzabal, J., Leal, J.F., Albarán, M.I., Lima, F.R., Pequeño, B., Ajenjo, N., Becerra, M., Alfonso, P., et al. (2011). Pim 1 kinase inhibitor ETP-45299 suppresses cellular proliferation and synergizes with PI3K inhibition. Cancer Lett. *300*, 145–153.
15. Gao, Y., Li, T., Wu, C., Bittle, G.J., Chen, S., Wu, Z.J., and Griffith, B.P. (2013). Pim-1 mediated signaling during the process of cardiac remodeling following myocardial infarction in ovine hearts. J. Mol. Cell. Cardiol. *63*, 89–97.
16. Din, S., Mason, M., Völkers, M., Johnson, B., Cottage, C.T., Wang, Z., Joyo, A.Y., Quijada, P., Erhardt, P., Magnuson, N.S., et al. (2013). Pim-1 preserves mitochondrial morphology by inhibiting dynamin-related protein 1 translocation. Proc. Natl. Acad. Sci. USA *110*, 5969–5974.
17. Liu, J.D., Chen, H.J., Wang, D.L., Wang, H., and Deng, Q. (2017). Pim-1 Kinase Regulating Dynamics Related Protein 1 Mediates Sevoflurane Postconditioning-induced Cardioprotection. Chin. Med. J. *130*, 309–317.
18. Mozaffari, M.S., Liu, J.Y., Abebe, W., and Baban, B. (2013). Mechanisms of load dependency of myocardial ischemia reperfusion injury. Am. J. Cardiovasc. Dis. *3*, 180–196.
19. Peralta, C., Jiménez-Castro, M.B., and Gracia-Sancho, J. (2013). Hepatic ischemia and reperfusion injury: effects on the liver sinusoidal milieu. J. Hepatol. *59*, 1094–1106.
20. Lentsch, A.B., Kato, A., Yoshidome, H., McMasters, K.M., and Edwards, M.J. (2000). Inflammatory mechanisms and therapeutic strategies for warm hepatic ischemia/reperfusion injury. Hepatology *32*, 169–173.
21. Eltzschig, H.K., and Eckle, T. (2011). Ischemia and reperfusion–from mechanism to translation. Nat. Med. *17*, 1391–1401.

22. Zhai, Y., Busuttil, R.W., and Kupiec-Weglinski, J.W. (2011). Liver ischemia and reperfusion injury: new insights into mechanisms of innate-adaptive immune-mediated tissue inflammation. Am. J. Transplant. *11*, 1563–1569.
23. Dery, K.J., Yao, S., Cheng, B., and Kupiec-Weglinski, J.W. (2023). New therapeutic concepts against ischemia-reperfusion injury in organ transplantation. Expert Rev. Clin. Immunol. *19*, 1205–1224.
24. Ikeda, T., Yanaga, K., Kishikawa, K., Kakizoe, S., Shimada, M., and Sugimachi, K. (1992). Ischemic injury in liver transplantation: difference in injury sites between warm and cold ischemia in rats. Hepatology *16*, 454–461.
25. Yang, X., Qin, L., Liu, J., Tian, L., and Qian, H. (2012). 17β-Estradiol protects the liver against cold ischemia/reperfusion injury through the Akt kinase pathway. J. Surg. Res. *178*, 996–1002.
26. Banerjee, S., Lu, J., Cai, Q., Sun, Z., Jha, H.C., and Robertson, E.S. (2014). EBNA3C augments Pim-1 mediated phosphorylation and degradation of p21 to promote B-cell proliferation. PLoS Pathog. *10*, e1004304.
27. Warfel, N.A., and Kraft, A.S. (2015). PIM kinase (and Akt) biology and signaling in tumors. Pharmacol. Ther. *151*, 41–49.
28. Yang, J., Liu, K., Yang, J., Jin, B., Chen, H., Zhan, X., Li, Z., Wang, L., Shen, X., Li, M., et al. (2017). PIM1 induces cellular senescence through phosphorylation of UHRF1 at Ser311. Oncogene *36*, 4828–4842.
29. Hu, S., Yan, G., Xu, H., He, W., Liu, Z., and Ma, G. (2014). Hypoxic preconditioning increases survival of cardiac progenitor cells via the pim-1 kinase-mediated anti-apoptotic effect. Circ. J. *78*, 724–731.
30. Velazquez, R., Shaw, D.M., Caccamo, A., and Oddo, S. (2016). Pim1 inhibition as a novel therapeutic strategy for Alzheimer's disease. Mol. Neurodegener. *11*, 52.
31. Zhu, N., Yi, B., Guo, Z., Zhang, G., Huang, S., Qin, Y., Zhao, X., and Sun, J. (2018). Pim-1 Kinase Phosphorylates Cardiac Troponin I and Regulates Cardiac Myofilament Function. Cell. Physiol. Biochem. *45*, 2174–2186.
32. Jackson, L.J., Pheneger, J.A., Pheneger, T.J., Davis, G., Wright, A.D., Robinson, J.E., Allen, S., Munson, M.C., and Carter, L.L. (2012). The role of PIM kinases in human and mouse CD4+ T cell activation and inflammatory bowel disease. Cell. Immunol. *272*, 200–213.
33. Kim, J.H., Kim, W.S., Yun, Y., and Park, C. (2010). Epstein-Barr virus latent membrane protein 1 increases chemo-resistance of cancer cells via cytoplasmic sequestration of Pim-1. Cell. Signal. *22*, 1858–1863.
34. Kumar, J.K., Ping, R.Y.S., Teong, H.F., Goh, S., and Clément, M.V. (2011). Activation of a non-genomic Pim-1/Bad-Pser75 module is required for an efficient pro-survival effect of Bcl-xL induced by androgen in LNCaP cells. Int. J. Biochem. Cell Biol. *43*, 594–603.
35. Hu, X.F., Li, J., Vandervalk, S., Wang, Z., Magnuson, N.S., and Xing, P.X. (2009). PIM-1-specific mAb suppresses human and mouse tumor growth by decreasing PIM-1 levels, reducing Akt phosphorylation, and activating apoptosis. J. Clin. Invest. *119*, 362–375.
36. Borillo, G.A., Mason, M., Quijada, P., Völkers, M., Cottage, C., McGregor, M., Din, S., Fischer, K., Gude, N., Avitabile, D., et al. (2010). Pim-1 kinase protects mitochondrial integrity in cardiomyocytes. Circ. Res. *106*, 1265–1274.
37. Meyer, J.N., Leuthner, T.C., and Luz, A.L. (2017). Mitochondrial fusion, fission, and mitochondrial toxicity. Toxicology *391*, 42–53.
38. Wang, K., Long, B., Zhou, L.Y., Liu, F., Zhou, Q.Y., Liu, C.Y., Fan, Y.Y., and Li, P.F. (2014). CARL lncRNA inhibits anoxia-induced mitochondrial fission and apoptosis in cardiomyocytes by impairing miR-539-dependent PHB2 downregulation. Nat. Commun. *5*, 3596.
39. Kiriyama, Y., and Nochi, H. (2017). Intra- and Intercellular Quality Control Mechanisms of Mitochondria. Cells *7*, 1.
40. Chang, C.R., and Blackstone, C. (2010). Dynamic regulation of mitochondrial fission through modification of the dynamin-related protein Drp1. Ann. N. Y. Acad. Sci. *1201*, 34–39.
41. Cereghetti, G.M., Stangherlin, A., Martins de Brito, O., Chang, C.R., Blackstone, C., Bernardi, P., and Scorrano, L. (2008). Dephosphorylation by calcineurin regulates translocation of Drp1 to mitochondria. Proc. Natl. Acad. Sci. USA *105*, 15803–15808.
42. Dickey, A.S., and Strack, S. (2011). PKA/AKAP1 and PP2A/Bβ2 regulate neuronal morphogenesis via Drp1 phosphorylation and mitochondrial bioenergetics. J. Neurosci. *31*, 15716–15726.
43. Shen, Y., Xie, Y., Zhao, Y., Long, Y., Li, L., and Zeng, Y. (2018). Pim-1 inhibitor attenuates trinitrobenzene sulphonic acid induced colitis in the mice. Clin. Res. Hepatol. Gastroenterol. *42*, 382–386.
44. Wei, X., Qian, J., Yao, W., Chen, L., Guan, H., Chen, Y., Xie, Y., Lu, H., Zhang, Z., Shi, L., and Lin, X. (2019). Hyperactivated peripheral invariant natural killer T cells correlate with the progression of HBV-relative liver cirrhosis. Scand. J. Immunol. *90*, e12775.
45. Pan, W.M., Wang, H., Zhang, X.F., Xu, P., Wang, G.L., Li, Y.J., Huang, K.P., Zhang, Y.W., Zhao, H., Du, R.L., et al. (2020). miR-210 Participates in Hepatic Ischemia Reperfusion Injury by Forming a Negative Feedback Loop With SMAD4. Hepatology *72*, 2134–2148.
46. Guan, G., Shen, Y., Yu, Q., Liu, H., Zhang, B., Guo, Y., Zhu, X., Li, Z., Rao, W., Zhuang, L., and Zang, Y. (2018). Down-regulation of IFIT3 protects liver from ischemia-reperfusion injury. Int. Immunopharmacol. *60*, 170–178.
47. Su, X., Chen, H., Zhu, Z., Xie, W., Peng, J., Ma, X., Jin, W., Shi, W., Deng, Z., and Li, C. (2021). Clinical Diagnostic Value of Quantitative Hepatitis B Virus Core Antibody Test in Chronic Viral Hepatitis B. Chronic Viral Hepatitis B *2021*, 3720571.
48. Guo, Y., Zhao, Y.R., Liu, H., Xin, Y., Yu, J.Z., Zang, Y.J., and Xu, Q.G. (2021). EHMT2 promotes the pathogenesis of hepatocellular carcinoma by epigenetically silencing APC expression. Cell Biosci. *11*, 152.
49. Xu, Q.G., Yuan, S.X., Tao, Q.F., Yu, J., Cai, J., Yang, Y., Guo, X.G., Lin, K.Y., Ma, J.Z., Dai, D.S., et al. (2019). A novel HBx genotype serves as a preoperative predictor and fails to activate the JAK1/STATs pathway in hepatocellular carcinoma. J. Hepatol. *70*, 904–917.
50. Xu, Q.G., Yu, J., Guo, X.G., Hou, G.J., Yuan, S.X., Yang, Y., Yang, Y., Liu, H., Pan, Z.Y., Yang, F., et al. (2018). IL-17A promotes the invasion-metastasis cascade via the AKT pathway in hepatocellular carcinoma. Mol. Oncol. *12*, 936–952.
51. Penna, C., Perrelli, M.G., Raimondo, S., Tullio, F., Merlino, A., Moro, F., Geuna, S., Mancardi, D., and Pagliaro, P. (2009). Postconditioning induces an anti-apoptotic effect and preserves mitochondrial integrity in isolated rat hearts. Biochim. Biophys. Acta *1787*, 794–801.
52. Keung, E.Z., Akdemir, K.C., Al Sannaa, G.A., Garnett, J., Lev, D., Torres, K.E., Lazar, A.J., Rai, K., and Chin, L. (2015). Increased H3K9me3 drives dedifferentiated phenotype via KLF6 repression in liposarcoma. J. Clin. Invest. *125*, 2965–2978.

STAR★METHODS

KEY RESOURCES TABLE

REAGENT or RESOURCE	SOURCE	IDENTIFIER
Antibodies		
PIM-1	Abcam	#ab308006
Caspase3	Cell Signaling	#9662
Cleaved Caspase3	Cell Signaling	#9664
β-actin	Proteintech	#66009-1-Ig
p-Drp1	Cell Signaling	#3455
T-Drp1	Cell Signaling	#8570
H3K9me3	Abcam	#ab8898
COX IV	Affinity	#AF5468
H3	Cell Signaling	#4499
Bax	Affinity	#AF0120
Bcl-2	Affinity	#AF6139
Cytc c	Cell Signaling	#11940
Mff	Abcam	#ab129075
Fis1	Abcam	# ab156865
Chemicals, peptides, and recombinant proteins		
DMEM	Cas9X	#GUMD-B301
Penicillin-Streptomycin	Solarbio	#P1400
Trypsin-EDTA	Solarbio	#T1320
Fetal Bovine Serum	Cas9X	#FBP-C520
Lipofectamine 3000	ThermoFisher	#L3000001
TCS PIM-1 1	Medchem express	#HY-18086
TRIzol reagent	Invitrogen	#15596026CN
DMSO	Solarbio	#D8371
Oligonucleotides		
Pim-1(H) qPCR Forward Primer	GGCTCGGTCTACTCAGGCA	
Pim-1(H) qPCR Reverse Primer	GGAAATCCGGTCCTTCTCCAC	
Pim-1(M) qPCR Forward Primer	TGCTCTTGTCCAAGATCAACTC	
Pim-1(M) qPCR Reverse Primer	CAGGGGCTCCTTCTCTTTGC	
Critical commercial assays		
Tunel Assay Kit	Elabscience	#E-CK-A321&E-CK-A322
H&E staing Kit	Beyotime	#C0105S
ALT Assay Kit	NJBI	#C009-2-1
AST Assay Kit	NJBI	#C010-2-1
BCA Protein Assay Kit	Solarbio	#PC0020
BeyoECL Plus	Beyotime	#P0018S
Experimental models: Cell lines/animals		
MIHA	FENGHUISHENGWU	#CL-0469
C57BL/6J	Experimental Animal Center of Qingdao University	N/A

(*Continued on next page*)

Continued

REAGENT or RESOURCE	SOURCE	IDENTIFIER
Software and algorithms		
Prsim10	Graphpad	https://www.graphpad.com/scientificsoftware/prism
ImageJ	N/A	https://imagej.net/ij/

RESOURCE AVAILABILITY

Lead contact

Further information and requests for resources and reagents should be directed to and will be fulfilled by the lead contact, Jinzhen Cai (caijinzhen@qdu.edu.cn).

Materials availability

Cell lines generated in this study are available upon request to the lead contact.

Data and code availability

- Data reported in this paper will be shared by the lead contact upon request.
- This paper does not report original code.
- Any additional information required to reanalyze the data reported in this paper is available from the lead contact upon request.

EXPERIMENTAL MODEL AND STUDY PARTICIPANT DETAILS

Clinical specimens

All experiments involving human specimens were approved by the Ethics Committee of the Affiliated Hospital of Qingdao University. Tissue and serum samples were collected from patients (male: $n = 14$; female: $n = 6$) receiving liver transplantation at the Affiliated Hospital of Qingdao University from January 2021 to January 2022. Liver tissues were obtained from liver grafts before liver transplantation and after hepatic artery reperfusion. The tissue and blood samples used in the present study were handled according to the guidelines outlined in the Declaration of Helsinki. All individual participants or families were thoroughly informed regarding the study and were asked to sign a written informed consent form.

Experimental animals

Suitable male C57BL/6J mice (purchased from the Experimental Animal Center of Qingdao University) weighing 23–27 g and aged 6–8 weeks were used in this study. The animals were raised in the Animal Experimental Center of Qingdao University and kept in a specific-pathogen-free (SPF) enclosure with a constant temperature and humidity and alternating light and dark for 12 h. All animal experiments complied with the regulations of the National Institutes of Health on the use and care of animals and were approved by the Animal Ethics Committee of Qingdao University.

Mouse model of hepatic ischemia–reperfusion and drug treatment

The mice were anesthetized with isoflurane, the skin was disinfected, and a median abdominal incision was made in the abdominal cavity to separate the portal vein branches and hepatic artery of the hepatic pedicle of the left and middle lobes of the liver. The portal vein branches and hepatic arteries of the hepatic pedicle of the left and middle lobes of the liver were clamped with a noninvasive vascular clamp. After continuous ischemia for 1 h, the vascular clamp was released to restore blood flow.[43] The mice were anesthetized at 0, 6, 12, and 24 h after reperfusion. Blood and liver samples were taken and preserved until further use. The Pim-1 inhibitor (TCS Pim-1 1) HY-18086 (MedChemExpress) was dissolved in 0.5% DMSO.[44] The mice were randomly divided into three groups: a sham operation group, a control group and an experimental group. The sham group was intraperitoneally injected with 0.5% DMSO solution. The control group was intraperitoneally injected with 0.5% DMSO solution for 5 days, while the experimental group was intraperitoneally injected with 5 mg/kg TCS PIM-1 for 5 days, and then the control and experimental groups were used to establish the mouse hepatic IR model.

Cell culture and transfection

The immortalized human hepatocyte MIHA cell line,[45] derived from Qingdao University, was cultured in high-glucose Dulbecco's modified Eagle medium (DMEM) containing 10% fetal bovine serum (FBS) and a 1% penicillin and/or streptomycin mixture. Cells were transiently transfected with Lipofectamine 3000 for MIHA cell lines or with polyetherimide for MIHA cell lines according to the manufacturer's instructions. Lentivirus production and small interference RNA was performed by Obio Technology Company (Shanghai, China). All stable MIHA cell lines

infected with lentivirus harboring Pim-1 overexpression constructs were treated with 0.5–2 μg/mL puromycin dihydrochloride for 7 days, and selected clones were confirmed as positive by PCR. Small interfering RNAs and their respective negative control RNAs were introduced into cells at 75 pmol per well of six-well plate according to the manufacturer's instructions.

Hypoxia/reoxygenation (HR) model

Cells were cultured at 37°C, and the concentration of CO^2 was kept at 5%, while the concentration of O^2 was 1%. After 1 h of hypoxia, the normal high-glucose DMEM containing 10% serum was replaced, and the cells were cultured in a normal incubator.[46] Cell protein or RNA was extracted after the cells had been reoxygenated for 0, 2, 6, and 12 h.

Western Blot (WB)

Cells were washed with PBS and collected. RIPA lysate and protease inhibitor were added for ice lysis. Mouse livers were collected, RIPA lysis buffer and protease inhibitor were added, and the samples were ground and lysed on ice. Total protein was quantified by the BCA method (Solarbio, Beijing, China). Protein (30 μg) was isolated by sodium dodecyl sulfate–polyacrylamide gel electrophoresis (SDS–PAGE). The protein was then transferred to a PVDF membrane (Millipore, Billerica, MA, USA) and blocked with 5% skim milk for 1 h. Diluted primary antibody (1:1000) was incubated at 4°C for 12 h and washed with TBST 3 times for 10 min. Then, the membrane was coupled with HRP secondary antibody (1:2000) and incubated at room temperature for 2 h. After the application of enhanced chemiluminescence reagent (ECL; Beyotime, China), the membrane was then rinsed with TBST three times for 10 min. Image Lab 4.1 and ImageJ software programs were used for quantitative western blotting of strips. Antibody: Pim-1 (ab308006, 1:1000, Abcam; 54523, 1:1000, CST); cleaved-caspase3 (9664, 1:1000, CST); caspase3 (9662, 1:1000, CST); β-actin (66009-1-Ig, 1:5000, Proteintech); Bax (AF0120, 1:3000, Affinity); Bcl2 (AF6139, 1:2000, Affinity); p-Drp1 (3455, 1:1000, CST); T-Drp1 (8570, 1:1000, CST); Cyt c (11940, 1:1000, CST); Mff (ab129075, 1:10000, Abcam); Fis1 (ab156865, 1:10000, Abcam); and COX-IV(AF5468, 1:2000, Affinity); and Ki-67 (ab16667, 1:1000, Abcam).

ALT and AST detection

Whole blood was centrifuged at 2500 rpm for 15 min. Serum ALT and AST levels were measured according to the instructions of the automated chemistry analyzer (Hitachi Labospect 008 AS, Japan).[47]

Quantitative reverse transcription polymerase chain reaction (qRT–PCR)

Total RNA was extracted from hepatocytes using TRIzol reagent (Invitrogen, USA). Reverse transcription of RNA into cDNA was performed using GoScript Reverse Transcription Mix (Promega, USA) according to the manufacturer's instructions. The cDNA was then detected using the GoTaq qPCR Master Mix reagent (Promega, USA). The PCR procedure consisted of 2 min at 94°C, 30 s at 94°C, 30 s at 56°C, 30 s at 72°C, 30 s at 72°C, and 5 min at 72°C. The primer sequences were listed as follows. Pim-1 (human): forward, GGCTCGGTCTACTCAGGCA; reverse, GGAAATCCGGTCCTTCTCCAC. Pim-1 (mouse): forward, TGCTCTTGTCCAAGATCAACTC; reverse, CAGGGGCTCCTTCTCTTTGC. CT values were calculated using automatically set thresholds and baselines, and CT values greater than 38 were excluded from the analysis.[48]

Immunohistochemical staining

For antigen repair, endogenous peroxidase was blocked using 3% hydrogen peroxide solution at room temperature for a 25 min incubation. Serum blocking was performed with 3% BSA for 30 min at room temperature. Primary antibody was added and incubated overnight in a wet box at 4°C. Secondary antibody was then added and incubated at room temperature for 1 h. For DAB color rendering, hematoxylin was used to stain the nuclei for 3 min. Slides were then dehydrated and sealed. Under the microscope, the positive areas were brownish yellow.[49]

Hematoxylin and eosin (H&E) staining

Liver tissue specimens were fixed with 10% formalin for 24 h and embedded in paraffin. Sections were stained with hematoxylin and eosin. The stained sections were examined by a pathologist using an Olympus light microscope, and were graded according to Suzuki's standards. In this classification, three indicators of liver injury – hepatic sinusoidal capillary congestion (score: 0–4), hepatocyte necrosis (score: 0–4), and balloon-like degeneration (score: 0–4) were graded and added to the total score (score: 0–12). The score was 0 for no congestion, necrosis, or balloon-like degeneration, and 12 for severe congestion/balloon-like degeneration and >60% lobular necrosis. Histological changes were assessed in randomly selected areas at 200x magnification.[50]

Terminal deoxynucleotidyl transferase dUTP nick end labeling (TUNEL) assay

For cell death, we used a One-step TUNEL *In Situ* Apoptosis Kit (E-CK-A321&E-CK-A322, Elabscience). Paraffin sections and cells in 24-well plates were treated according to the instructions, and then photos were taken with a fluorescence microscope.

Transmission electron microscopy (TEM)

Tissue slices and cell smears were fixed in 2.5% glutaraldehyde solution. The samples were treated with standard procedures such as dehydration, embedding and sectioning and then examined and photographed under a Hitachi 7500 transmission electron microscope.[51] Mitochondrial morphology was quantified using Fiji/ImageJ software.

Chromatin immunoprecipitation assay (ChIP)

ChIP sequencing was outsourced to Kangcheng Biotechnology (Shanghai, China), completing with a previously described operating procedure.[52] Briefly, cells transfected with relative plasmids were cross-linked using 1% formaldehyde at 37°C for 10 min. After washing with PBS, the cells were resuspended in 300 μL of lysis buffer (50 mM Tris (pH 8.1), 10 mM EDTA, 1% SDS, and 1 mM PMSF). DNA was sheared into small fragments by sonication. The supernatants were precleared using herring sperm DNA/protein G-Sepharose slurry (Sigma–Aldrich, USA). The recovered supernatants were incubated with specific antibody or an isotype control IgG for 2 h in the presence of herring sperm DNA and protein G-Sepharose beads. The immunoprecipitated DNA was retrieved from the beads with 1% SDS and a 1.1 M NaHCO3 solution at 65°C for 6 h. DNA was then purified using a PCR purification kit (Qiagen, USA).

Separation of mitochondria and cytoplasmic proteins

2.5mL of PMSF-added mitochondrial separation reagent (C3601, Beyotime) was added to 50 million cells, gently suspended and placed in an ice bath for 10–15 min. Transfer the cell suspension to a glass homogenizer of appropriate size, homogenize about 10–30 times. Cell homogenates were centrifuged at 600g and 4°C for 10 min. Leave the supernatant at 11,000g and centrifuge at 4°C for 10 min. The precipitated cell mitochondria were isolated. The supernatant collected was 12,000g and centrifuged at 4°C for 10 min. The supernatant is the cytoplasmic protein that removes mitochondria.

QUANTIFICATION AND STATISTICAL ANALYSIS

SPSS statistical software was used for analysis, and the measurement data are expressed as the mean ± standard deviation. For comparisons, Student's t test and the Mann–Whitney U test were performed as appropriate. Pearson's analysis was performed for the correlation analysis. $p < 0.05$ was considered statistically significant.